Results in Applied Mathematics 8 (2020) 100097

Contents lists available at ScienceDirect

Results in Applied Mathematics

journal homepage: www.elsevier.com/locate/results-in-applied-mathematics

Stabilizer-free weak Galerkin methods for monotone quasilinear elliptic PDEs

Xiu Ye [a], Shangyou Zhang [b], Yunrong Zhu [c,*]

[a] Department of Mathematics, University of Arkansas at Little Rock, Little Rock, AR 72204, United States of America
[b] Department of Mathematical Sciences, University of Delaware, Newark, DE 19716, United States of America
[c] Department of Mathematics and Statistics, Idaho State University, Pocatello, ID 83209, United States of America

ARTICLE INFO

Article history:
Received 27 November 2019
Received in revised form 31 January 2020
Accepted 10 February 2020
Available online 22 February 2020

MSC:
65N30
35J62

Keywords:
Uniqueness
Monotone PDEs
Quasilinear equations
Weak Galerkin methods
Stabilizer-free

ABSTRACT

In this paper, we study the stabilizer-free weak Galerkin methods on polytopal meshes for a class of second order elliptic boundary value problems of divergence form and with gradient nonlinearity in the principal coefficient. With certain assumptions on the nonlinear coefficient, we show that the discrete problem has a unique solution. This is achieved by showing that the associated operator satisfies certain continuity and monotonicity properties. With the help of these properties, we derive optimal error estimates in the energy norm. We present several numerical examples to verify the error estimates.

1. Introduction

We consider the stabilizer free weak Galerkin method for the quasilinear elliptic partial differential equations (PDEs) in $\Omega \subset \mathbb{R}^d$ with $d = 2$, or 3:

$$\begin{cases} -\nabla \cdot (\kappa(x, |\nabla u|)\nabla u) &= f \quad \text{in } \Omega, \\ u &= 0 \quad \text{on } \partial\Omega. \end{cases} \tag{1.1}$$

This class of PDEs arise, for example, in the study of compressible flow in the airfoil design (cf. [1]) or the eddy currents in a nonlinear ferromagnetic material (cf. [2]). We assume throughout the paper that the diffusion coefficient $\kappa(x, s)$, for $x \in \Omega$ and $s \in \mathbb{R}$ satisfies the following assumption.

Assumption 1.1. Assume $\kappa(x, s)$ is a Carathéodory function, and assume that there are constants $0 < \alpha < \beta$ with

$$\alpha(t - s) \le \kappa(x, t)t - \kappa(x, s)s \le \beta(t - s), \quad 0 \le s \le t \tag{1.2}$$

for a.e. $x \in \Omega$.

* Corresponding author.
E-mail addresses: xxye@ualr.edu (X. Ye), szhang@udel.edu (S. Zhang), zhuyunr@isu.edu (Y. Zhu).

https://doi.org/10.1016/j.rinam.2020.100097

Note that this assumption implies that $\alpha \le \kappa(x,t) \le \beta$ a.e. $x \in \Omega$ and for all $t > 0$. For simplicity, we denote $\kappa(s) := \kappa(x,s)$ in the rest of paper.

The analysis of standard conforming finite element method for general quasilinear problems was discussed in [3]. For the class of monotone quasilinear PDEs (1.1), the finite element error estimates were developed in [4] for the differential operators defined on a reflexive Banach space. In [5], a one-parameter family of *hp*-version discontinuous Galerkin finite element methods was developed and analyzed for the numerical approximation of this type of quasilinear elliptic equations, subject to mixed Dirichlet–Neumann boundary conditions on $\partial\Omega$. The finite volume methods were discussed in [6].

First proposed in [7], the weak Galerkin (WG) finite element methods are based on the novel idea of using *weak functions* and their *weak derivative* (see Section 2 for more details) in the design of numerical approximation schemes. Due to the discontinuous nature of the methods, the WG methods are very flexible in solving a variety of PDEs on general polytopal meshes. For the second order elliptic quasilinear PDEs, the existence of solutions of the WG methods was shown in [8] by a Schauder fixed point argument. However, the uniqueness and the error estimations of the numerical approximations are restricted only to the linear PDEs, and have not been addressed for the nonlinear ones. Only recently in [9], the authors gave the well-posedness and error estimate in the energy norm for the monotone quasilinear PDEs (1.1).

One disadvantage of the aforementioned WG methods, as well as other classes of discontinuous finite element methods (e.g. discontinuous Galerkin methods), is the existence of stabilization terms, which are usually necessary to enforce weak continuity of the discontinuous solutions across element boundaries. Removing stabilizers from discontinuous finite element methods will simplify formulations and reduce programming complexity significantly. Motivated by this, a class of stabilizer-free WG methods were first proposed and analyzed recently in [10] for Poisson's equation. In this new formulation, the WG methods can be viewed as the counterpart of the weak formulation of the continuous problem by replacing the classical gradient by the weak gradient operator.

The goal of this paper is to formulate and analyze this stabilizer-free WG methods for the monotone quasilinear PDEs (1.1). With the structural Assumption 1.1, we show the stabler-free WG formulation satisfies certain continuity and monotonicity properties. These properties imply the discrete problem has a unique solution, thanks to a nonlinear version of the Lax–Milgram theorem (Theorem 3.1) for monotone operators. We then derive optimal error estimates in the energy norm.

The rest of this paper is organized as follows. In Section 2, we introduce basic notation, and present the stabilizer-free WG methods for the model problem (1.1). In Section 3, we discuss the existence and uniqueness of the discrete problem. We first present an abstract existence and uniqueness of nonlinear operator equation, then verify the stabilizer-free WG methods satisfies the conditions based on Assumption 1.1. In Section 4, we show the main error estimate in the energy norm. In Section 5, we present some numerical experiments to confirm the theory. The paper ends with some concluding remarks and prospects for future work.

2. Weak Galerkin method

For any given subset $D \subseteq \Omega$, we use the standard definition of Sobolev spaces $H^s(D)$ with $s \ge 0$. The associated inner product, norm, and semi-norms in $H^s(D)$ are denoted by $(\cdot,\cdot)_{s,D}$, $\|\cdot\|_{s,D}$, and $|\cdot|_{s,D}$, respectively. When $s = 0$, $H^0(D)$ coincides with the space of square integrable functions $L^2(D)$. In this case, the subscript s is suppressed from the notation of norm, semi-norm, and inner products. Furthermore, the subscript D is also suppressed when $D = \Omega$. Throughout the paper, we use C to denote a generic positive constant that is independent of the meshsize and the solutions, and may take different values in different appearance.

Let $\mathcal{T}_h$ be a partition of the domain Ω consisting of polygons in two dimensions or polyhedra in three dimensions satisfying a set of shape-regular conditions (see [8] for example). For every element $T \in \mathcal{T}_h$, we denote by h_T the diameter of T and mesh size $h := \max_{T\in\mathcal{T}_h} h_T$ for $\mathcal{T}_h$.

We introduce the *weak function* $v = \{v_0, v_b\}$ that allows v to take different forms in the interior and on the boundary of each element $T \in \mathcal{T}_h$:

$$v = \begin{cases} v_0, & \text{in } T, \\ v_b, & \text{on } \partial T. \end{cases}$$

Given an integer $k \ge 1$, we define a local finite element space $V_h(T)$ on each element $T \in \mathcal{T}_h$ as follows

$$V_h(T) = \{v = \{v_0, v_b\} : v_0 \in \mathbb{P}_k(T),\ \ v_b|_e \in \mathbb{P}_k(e), e \in \partial T\}. \tag{2.1}$$

A global finite element space V_h is then derived by patching all the local elements $V_h(T)$ with common values on interior edges. Let V_h^0 be a subspace of V_h consisting of functions with vanishing boundary.

For any $v = \{v_0, v_b\}$, the *discrete weak gradient* $\nabla_w v \in [\mathbb{P}_j(T)]^d$ is defined as the unique vector field satisfying

$$(\nabla_w v,\ \boldsymbol{\tau})_T = -(v_0,\ \nabla\cdot\boldsymbol{\tau})_T + \langle v_b, \boldsymbol{\tau}\cdot\boldsymbol{n}\rangle_{\partial T}, \quad \forall \boldsymbol{\tau} \in [\mathbb{P}_j(T)]^d, \tag{2.2}$$

where $j > k$ is an integer to be specified later (see Lemma 2.1). For simplicity, we adopt the following notations,

Then the WG scheme for (1.1) is to find $u_h = \{u_0, u_b\} \in V_h^0$ such that:

$$a_h(u_h; u_h, v) := (\kappa(|\nabla_w u_h|)\nabla_w u_h, \nabla_w v)_{\mathcal{T}_h} = (f,\ v_0) \quad \forall v = \{v_0, v_b\} \in V_h^0. \tag{2.3}$$

Let Q_0, Q_b and $\mathbb{Q}_h$ be the locally defined L^2 projections onto $\mathbb{P}_k(T)$, $\mathbb{P}_k(e)$ and $[\mathbb{P}_j(T)]^d$ accordingly on each element $T \in \mathcal{T}_h$ and $e \subset \partial T$. For the exact solution u of (1.1), we define $Q_h u$ as

$$Q_h u = \{Q_0 u, Q_b u\} \in V_h.$$

For any $v \in V_h + H^1(\Omega)$, we introduce the following energy norm and the corresponding inner product:

$$|||v|||^2 = (\nabla_w v, \nabla_w v)_{\mathcal{T}_h}. \tag{2.4}$$

We also define a discrete H^1 semi-norm as follows:

$$\|v\|_{1,h} = \left(\sum_{T \in \mathcal{T}_h} \left(\|\nabla v_0\|_T^2 + h_T^{-1} \|v_0 - v_b\|_{\partial T}^2 \right) \right)^{\frac{1}{2}}. \tag{2.5}$$

It is easy to see that $\|v\|_{1,h}$ defines a norm in V_h^0. The following lemma indicates that $\|\cdot\|_{1,h}$ is equivalent to the $|||\cdot|||$ in (2.4).

Lemma 2.1 ([10,11]). *Let $j = n + k - 1$, where n is the number of edges (faces) in each element. There exist two positive constants C_1 and C_2 such that for any $v = \{v_0, v_b\} \in V_h$, we have*

$$C_1 \|v\|_{1,h} \le |||v||| \le C_2 \|v\|_{1,h}. \tag{2.6}$$

We remark that even though in Lemma 2.1 we required $j = n+k-1$, our numerical experiments in Section 5 indicate that we can still get optimal error estimates with $j = k + 1$ or $j = k + 2$.

3. Existence and uniqueness

In this section, we show the problem (2.3) has a unique solution. For this purpose, we first present an abstract theorem. Let H be a Hilbert space with the inner product denoted by $(\cdot, \cdot)_H$ and the induced norm $\|\cdot\|_H$. We say a (nonlinear) operator $N : H \to H$ is *strongly monotone* if there exists a constant $\lambda > 0$ such that

$$(N(u) - N(v), u - v)_H \ge \lambda \|u - v\|_H^2; \tag{3.1}$$

$N : H \to H$ is *Lipschitz continuous* if there is a constant $\Lambda > 0$ such that

$$\|N(u) - N(v)\|_H \le \Lambda \|u - v\|_H. \tag{3.2}$$

The following theorem (cf. [12]) can be viewed as the nonlinear version of the Lax–Milgram theorem. For completeness, we include a simple proof here.

Theorem 3.1. *Let the operator $N : H \to H$ be strongly monotone (3.1) and Lipschitz continuous (3.2). Then $N(u) = f$ has a unique solution for all $f \in H$.*

Proof. Let $Au = u - \varepsilon(N(u) - f)$. It is clear that the solution to the equation $N(u) = f$ is equivalent to the fixed point $Au = u$ of A. By the strong monotonicity (3.1) and Lipschitz continuity (3.2), the operator $A : H \to H$ satisfies

$$\begin{aligned} \|Au - Av\|_H^2 &= \|u - v\|_H^2 + \varepsilon^2 \|N(u) - N(v)\|_H^2 - 2\varepsilon (N(u) - N(v), u - v)_H \\ &\le \left(1 - 2\varepsilon\lambda + \Lambda\varepsilon^2\right) \|u - v\|_H^2. \end{aligned}$$

Clearly, for any $\varepsilon \in (0, 2\lambda/\Lambda^2)$, $A : H \to H$ is a contraction mapping. By Banach fixed-point theorem, A has a unique fixed point. Hence $N(u) = f$ has a unique solution. □

Remark 3.2. By the proof of Theorem 3.1, we can construct a fixed point iteration $u_{n+1} = Au_n$ for any initial guess $u_0 \in H$. For appropriate choice of ε, this iteration is guaranteed to converge (globally). This is in fact the relaxed Picard iteration, which is the algorithm used in Section 5 for solving the nonlinear problems.

Based on Theorem 3.1, in order to show (2.3) has a unique solution, we just need to verify the related discrete nonlinear operator satisfies the strong monotonicity (3.1) and the Lipschitz continuity (3.2). These properties can be obtained by Assumption 1.1 on the coefficient κ. We first show the following continuity and monotonicity lemma.

Lemma 3.3. *If the coefficient κ satisfies Assumption 1.1, then we have*

$$\alpha |\boldsymbol{\xi} - \boldsymbol{\eta}|^2 \le (\kappa(|\boldsymbol{\xi}|)\boldsymbol{\xi} - \kappa(|\boldsymbol{\eta}|)\boldsymbol{\eta}, \boldsymbol{\xi} - \boldsymbol{\eta}), \qquad \forall \boldsymbol{\xi}, \boldsymbol{\eta} \in \mathbb{R}^d \tag{3.3}$$

$$|\kappa(|\boldsymbol{\xi}|)\boldsymbol{\xi} - \kappa(|\boldsymbol{\eta}|)\boldsymbol{\eta}| \le \beta |\boldsymbol{\xi} - \boldsymbol{\eta}|, \qquad \forall \boldsymbol{\xi}, \boldsymbol{\eta} \in \mathbb{R}^d. \tag{3.4}$$

Proof. To prove (3.3), we use the lower bound in Assumption 1.1.

$$\begin{aligned}
&(\kappa(|\boldsymbol{\xi}|)\boldsymbol{\xi} - \kappa(|\boldsymbol{\eta}|)\boldsymbol{\eta}, \boldsymbol{\xi} - \boldsymbol{\eta}) = \kappa(|\boldsymbol{\xi}|)|\boldsymbol{\xi}|^2 + \kappa(|\boldsymbol{\eta}|)|\boldsymbol{\eta}|^2 - [\kappa(|\boldsymbol{\xi}|) + \kappa(|\boldsymbol{\eta}|)]\boldsymbol{\xi}\cdot\boldsymbol{\eta} \\
&= (\kappa(|\boldsymbol{\xi}|)|\boldsymbol{\xi}| - \kappa(|\boldsymbol{\eta}|)|\boldsymbol{\eta}|)(|\boldsymbol{\xi}| - |\boldsymbol{\eta}|) + [\kappa(|\boldsymbol{\xi}|) + \kappa(|\boldsymbol{\eta}|)](|\boldsymbol{\xi}||\boldsymbol{\eta}| - \boldsymbol{\xi}\cdot\boldsymbol{\eta}) \\
&\geq \alpha(|\boldsymbol{\xi}| - |\boldsymbol{\eta}|)^2 + 2\alpha(|\boldsymbol{\xi}||\boldsymbol{\eta}| - \boldsymbol{\xi}\cdot\boldsymbol{\eta}) \\
&= \alpha|\boldsymbol{\xi} - \boldsymbol{\eta}|^2.
\end{aligned}$$

On the other hand, by the upper bound in Assumption 1.1, we have,

$$\begin{aligned}
&|\kappa(|\boldsymbol{\xi}|)\boldsymbol{\xi} - \kappa(|\boldsymbol{\eta}|)\boldsymbol{\eta}|^2 = \kappa(|\boldsymbol{\xi}|)|\boldsymbol{\xi}|^2 + \kappa(|\boldsymbol{\eta}|)|\boldsymbol{\eta}|^2 - 2\kappa(|\boldsymbol{\xi}|)\kappa(|\boldsymbol{\eta}|)\boldsymbol{\xi}\cdot\boldsymbol{\eta} \\
&= (\kappa(|\boldsymbol{\xi}|)|\boldsymbol{\xi}| - \kappa(|\boldsymbol{\eta}|)|\boldsymbol{\eta}|)^2 + 2\kappa(|\boldsymbol{\xi}|)\kappa(|\boldsymbol{\eta}|)(|\boldsymbol{\xi}||\boldsymbol{\eta}| - \boldsymbol{\xi}\cdot\boldsymbol{\eta}) \\
&\leq \beta^2(|\boldsymbol{\xi}| - |\boldsymbol{\eta}|)^2 + 2\beta^2(|\boldsymbol{\xi}||\boldsymbol{\eta}| - \boldsymbol{\xi}\cdot\boldsymbol{\eta}) \\
&= \beta^2|\boldsymbol{\xi} - \boldsymbol{\eta}|^2.
\end{aligned}$$

Taking square root on both sides, we obtain (3.4). □

The estimate (3.3) in Lemma 3.3 implies the following strong monotonicity of a_h.

Lemma 3.4. *If the coefficient κ satisfies Assumption 1.1, then the nonlinear form a_h defined in (2.3) is strongly monotone in the sense that*

$$\alpha|||u_1 - u_2|||^2 \leq a_h(u_1; u_1, u_1 - u_2) - a_h(u_2; u_2, u_1 - u_2), \quad \forall u_1, u_2 \in V_h^0.$$

Proof. The conclusion is a direct consequence of the inequality (3.3). □

On the other hand, the estimate (3.4) implies the following Lipschitz continuity of a_h.

Lemma 3.5. *If the coefficient κ satisfies Assumption 1.1, then the nonlinear form a_h defined in (2.3) is Lipschitz continuous in the sense that*

$$|a_h(u_1; u_1, v) - a_h(u_2; u_2, v)| \leq \beta|||u_1 - u_2|||\,|||v|||, \qquad \forall u_1, u_2, v \in V_h^0.$$

Proof. By inequality (3.4), we immediately get that

$$\begin{aligned}
|a_h(u_1; u_1, v) - a_h(u_2; u_2, v)| &= \left|(\kappa(|\nabla_w u_1|)\nabla_w u_1 - \kappa(|\nabla_w u_2|)\nabla_w u_2, \nabla_w v)_{\mathcal{T}_h}\right| \\
&\leq \beta|||u_1 - u_2|||\,|||v|||.
\end{aligned}$$

This completes the proof. □

Now, we are ready to present the existence and uniqueness of (2.3).

Theorem 3.6. *If the coefficient κ satisfies Assumption 1.1, then the weak Galerkin finite element scheme (2.3) has a unique solution.*

Proof. In order to use the abstract existence and uniqueness result in Theorem 3.1, we first need to rewrite Eq. (2.3) in the operator form on the finite dimensional Hilbert space V_h^0 with the inner product and norm defined in (2.4). For any $v = \{v_0, v_b\} \in V_h^0$ we have (cf. [8, Lemma 7.1], and Lemma 2.1)

$$\|v_0\| \leq C\|v\|_{1,h} \leq C|||v|||. \tag{3.5}$$

Hence, we have

$$|(f, v_0)| \leq \|f\|\|v_0\| \leq C\|f\|\,|||v|||.$$

This implies that f is a bounded linear functional on V_h^0. Then by Riesz representation theorem, there exists an $\boldsymbol{f} \in V_h^0$ such that

$$(f, v) = \langle \boldsymbol{f}, v\rangle, \qquad \forall v \in V_h^0.$$

Here, $\langle\cdot,\cdot\rangle$ is the inner product defined in (2.4).

Fix a $w \in V_h^0$, consider the linear functional $\Phi_w(v) := a_h(w; w, v)$ for any $v \in V_h^0$. By Assumption 1.1, it is clear that

$$\Phi_w(v) \leq \beta|||w|||\,|||v|||.$$

That is, Φ_w is a bounded linear functional on V_h^0. By Riesz representation theorem, there exists a $N(w) \in V_h^0$ such that

$$\Phi_w(v) = \langle N(w), v\rangle, \qquad \forall v \in V_h^0.$$

Therefore, (2.3) is equivalent to the following operator form: Find $u_h \in V_h^0$ such that

$$N(u_h) = \boldsymbol{f}. \tag{3.6}$$

Lemma 3.4 implies that N is strongly monotone, and Lemma 3.5 implies that N is Lipschitz continuous on V_h^0. By Theorem 3.1, (3.6) has a unique solution. Therefore, (2.3) has a unique solution. □

4. Error analysis

In this section, we establish the error estimate for the WG finite element approximation (2.3) in the energy norm defined in (2.4). For this purpose, we first introduce the following lemmas.

Lemma 4.1 ([10, Lemma 2.1]). *Let $v \in H^1(\Omega)$, then on any element $T \in \mathcal{T}_h$, it holds*

$$\nabla_w v = \mathbb{Q}_h \nabla v. \tag{4.1}$$

Lemma 4.2 ([10, Lemma 4.3]). *Let $w \in H^{k+1}(\Omega)$. Then*

$$|||w - Q_h w||| \le Ch^k |w|_{k+1}. \tag{4.2}$$

Now we are ready to prove the main theorem.

Theorem 4.3. *Let $u_h \in V_h$ be the weak Galerkin finite element solution to (2.3). Assume that $u \in H^{k+1}(\Omega)$ is the exact solution to (1.1), and the coefficient κ satisfies Assumption 1.1. If in addition, $\kappa \in W^{k,\infty}(\Omega \times \mathbb{R}^+)$, then there exists a constant $C > 0$ independent of h, u and u_h such that*

$$|||u - u_h||| \le Ch^k \|u\|_{k+1}.$$

Proof. By (4.2) and the triangle inequality, it suffices to show that

$$|||u_h - Q_h u||| \le Ch^k |u|_{k+1}. \tag{4.3}$$

For simplicity, let $e_h := u_h - Q_h u = \{e_0, e_b\} \in V_h^0$, where $e_0 = u_0 - Q_0 u$ and $e_b = u_b - Q_b u$. We also denote $\boldsymbol{\sigma}(v) := \kappa(|\nabla v|)\nabla v$ and $\boldsymbol{\sigma}_w(v) := \kappa(|\nabla_w v|)\nabla_w v$.

We test the continuous equation (1.1) with v_0 for any $v = \{v_0, v_b\} \in V_h^0$. Notice that the flux $\boldsymbol{\sigma}(u)$ is continuous in the normal direction, we obtain

$$(\boldsymbol{\sigma}(u), \nabla v_0)_{\mathcal{T}_h} - \langle \boldsymbol{\sigma}(u) \cdot \boldsymbol{n}, v_0 - v_b \rangle_{\partial \mathcal{T}_h} = (f, v_0)_{\mathcal{T}_h}. \tag{4.4}$$

Then by the strong monotonicity Lemma 3.4, we have

$$\begin{aligned} \alpha |||e_h|||^2 &\le a_h(u_h; u_h, e_h) - a_h(Q_h u; Q_h u, e_h) \\ &= (f, e_0)_{\mathcal{T}_h} - a_h(Q_h u; Q_h u, e_h) \\ &= (\boldsymbol{\sigma}(u), \nabla e_0)_{\mathcal{T}_h} - \langle \boldsymbol{\sigma}(u) \cdot \boldsymbol{n}, e_0 - e_b \rangle_{\partial \mathcal{T}_h} - (\boldsymbol{\sigma}_w(Q_h u), \nabla_w e_h)_{\mathcal{T}_h}, \end{aligned} \tag{4.5}$$

where we used (4.4) in the last step. On each $T \in \mathcal{T}_h$, it follows from integration by parts and the definition of the discrete weak gradient (2.2),

$$\begin{aligned} (\boldsymbol{\sigma}(u), \nabla e_0)_T &= (\mathbb{Q}_h(\boldsymbol{\sigma}(u)), \nabla e_0)_T \\ &= -(\nabla \cdot \mathbb{Q}_h(\boldsymbol{\sigma}(u)), e_0)_T + \langle \mathbb{Q}_h(\boldsymbol{\sigma}(u)) \cdot \boldsymbol{n}, e_0 \rangle_{\partial T} \\ &= (\mathbb{Q}_h(\boldsymbol{\sigma}(u)), \nabla_w e_h)_T + \langle \mathbb{Q}_h(\boldsymbol{\sigma}(u)) \cdot \boldsymbol{n}, e_0 - e_b \rangle_{\partial T}. \end{aligned}$$

Therefore, we get

$$(\boldsymbol{\sigma}(u), \nabla e_0)_{\mathcal{T}_h} = (\mathbb{Q}_h(\boldsymbol{\sigma}(u)), \nabla_w e_h)_{\mathcal{T}_h} + \langle \mathbb{Q}_h(\boldsymbol{\sigma}(u)) \cdot \boldsymbol{n}, e_0 - e_b \rangle_{\partial \mathcal{T}_h}. \tag{4.6}$$

Replacing the first term on the right-hand side of the inequality (4.5) with the right-hand side of (4.6), we obtain

$$\begin{aligned} \alpha |||e_h|||^2 &\le (\mathbb{Q}_h(\boldsymbol{\sigma}(u)) - \boldsymbol{\sigma}_w(Q_h u), \nabla_w e_h)_{\mathcal{T}_h} \\ &\quad - \langle (\mathbb{Q}_h(\boldsymbol{\sigma}(u)) - \boldsymbol{\sigma}(u)) \cdot \boldsymbol{n}, e_0 - e_b \rangle_{\partial \mathcal{T}_h}. \end{aligned} \tag{4.7}$$

To estimate the first term in (4.7), we have

$$\begin{aligned} \|\mathbb{Q}_h(\boldsymbol{\sigma}(u)) - \boldsymbol{\sigma}_w(Q_h u)\| &\le \|(I - \mathbb{Q}_h)\boldsymbol{\sigma}(u)\| + \|\boldsymbol{\sigma}(u) - \boldsymbol{\sigma}_w(Q_h u)\| \\ &\le Ch^k |\boldsymbol{\sigma}(u)|_k + \beta \|\nabla u - \nabla_w(Q_h u)\| \\ &\le Ch^k |u|_{k+1} + \beta \left(\|\nabla u - \nabla_w u\| + \|\nabla_w(u - Q_h u)\|\right) \end{aligned}$$

$$= Ch^k|u|_{k+1} + \beta\,(\|\nabla u - \mathbb{Q}_h\nabla u\| + |||u - Q_h u|||)$$
$$\le Ch^k|u|_{k+1} \tag{4.8}$$

where in the second inequality we used the inequality (3.4), in the third inequality we used the condition $\kappa \in W^{k,\infty}(\Omega \times \mathbb{R}^+)$, and in the fourth equality we used Lemma 4.1 for the second term and the definition of the norm (2.4) for the last term. Here, we have also used the approximation properties for $\mathbb{Q}_h$ and Q_h in the last step. In particular, we have

$$\|\boldsymbol{q} - \mathbb{Q}_h\boldsymbol{q}\| \le Ch^k|\boldsymbol{q}|_k \tag{4.9}$$

(see [13, Lemma 4.1] for a proof of this inequality on general polytopal mesh); for the last term $|||u - Q_h u|||$, the estimate follows directly from (4.2). Therefore, we obtain the following estimate for the first term in (4.7)

$$(\mathbb{Q}_h(\boldsymbol{\sigma}(u)) - \boldsymbol{\sigma}_w(Q_h u), \nabla_w e_h)_{\mathcal{T}_h} \le \|\mathbb{Q}_h(\boldsymbol{\sigma}(u)) - \boldsymbol{\sigma}_w(Q_h u)\|\,|||e_h|||$$
$$\le Ch^k|u|_{k+1}|||e_h|||. \tag{4.10}$$

Now we turn to estimate the second term in (4.7). We need the following trace inequality for any function $v \in H^1(T)$ (cf. [13]):

$$\|v\|_{\partial T}^2 \le C(h_T^{-1}\|v\|_T^2 + h_T\|\nabla v\|_T^2). \tag{4.11}$$

By this trace inequality and the estimate (4.8), we have the following estimate for the second term in (4.7):

$$\langle(\mathbb{Q}_h(\boldsymbol{\sigma}(u)) - \boldsymbol{\sigma}(u)) \cdot \boldsymbol{n}, e_0 - e_b\rangle_{\partial\mathcal{T}_h}$$
$$\le C\sum_{T\in\mathcal{T}_h}\|\mathbb{Q}_h(\boldsymbol{\sigma}(u)) - \boldsymbol{\sigma}(u)\|_{\partial T}\|e_0 - e_b\|_{\partial T}$$
$$\le C\left(\sum_{T\in\mathcal{T}_h} h_T\|\mathbb{Q}_h(\boldsymbol{\sigma}(u)) - \boldsymbol{\sigma}(u)\|_{\partial T}^2\right)^{1/2}\left(\sum_{T\in\mathcal{T}_h} h_T^{-1}\|e_0 - e_b\|_{\partial T}^2\right)^{1/2}$$
$$\le Ch^k|\boldsymbol{\sigma}(u)|_k|||e_h||| \le Ch^k|u|_{k+1}|||e_h|||. \tag{4.12}$$

In the last inequality, we used the trace inequality (4.11), the estimate (4.9), the condition $\kappa \in W^{k,\infty}(\Omega \times \mathbb{R}^+)$, and the norm equivalency (2.6). The conclusion then follows directly from inequalities (4.10) and (4.12). This completes the proof. □

5. Numerical experiments

We apply the new stabilizer-free weak Galerkin finite element method with various polynomial degrees and on various polygonal grids, to two monotone elliptic equations. Even though we did not give the analysis for the L^2 error estimates, we present them in these numerical examples for comparison. Note the L^2 error between the exact solution $u \in H_0^1(\Omega)$ and the WG approximation $u_h = \{u_0, u_b\} \in V_h^0$ is defined by

$$\|u - u_h\|_0^2 := \sum_{T\in\mathcal{T}_h}\int_T |u - u_0|^2 dx.$$

5.1. Example 1

We solve problem (1.1) on square domain $\Omega = (0, 1)^2$, where the coefficient function and the exact solution are

$$\kappa(|\nabla u|) = 1 + e^{-|\nabla u|^2}, \quad u = \sin(\pi x)(y - y^2). \tag{5.1}$$

This function κ satisfies condition (1.2) with $\alpha = 1 - \sqrt{2/e}$ and $\beta = 2$.

We compute the solution (5.1) on two types of grids, shown in Figs. 1 and 2. We use $\mathbb{P}_k$ ($k = 1, 2, 3, 4$ in (2.1)) weak Galerkin finite elements with $\mathbb{P}_{k+1}$ weak gradient ($j = k + 1$) in (2.2) on rectangular grids (Fig. 1), and $\mathbb{P}_k$ ($k = 1, 2, 3$ in (2.1)) weak Galerkin finite elements with $\mathbb{P}_{k+2}$ weak gradient ($j = k + 2$) in (2.2) on polygonal grids (Fig. 2). In the computation, the function $\kappa(|\nabla u_h|)$ is interpolated in to the discontinuous $\mathbb{P}_{k-1}$ space on the same grid. On each level, we solve the nonlinear discrete equations by the relaxed-Picard iteration. The errors and the order of convergence are listed in Tables 1–2 for the computation on two types of grids, respectively.

For a comparison, we also solve this problem by the traditional weak Galerkin finite element method, i.e., the method with a stabilization/penalty. The WG with a stabilization is to find $u_h = \{u_0, u_b\} \in V_h^0$ such that:

$$(\kappa(|\nabla_w u_h|)\nabla_w u_h, \nabla_w v)_{\mathcal{T}_h} + \langle\frac{1}{h}(u_0 - u_b), v_0 - v_b\rangle_{\partial\mathcal{T}_h} = (f,\ v_0) \tag{5.2}$$

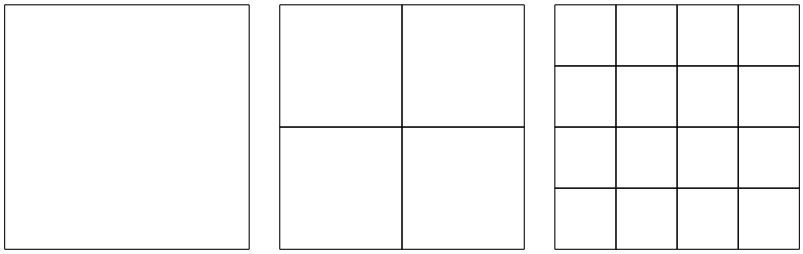

Fig. 1. The level one, level two and level three rectangular grids.

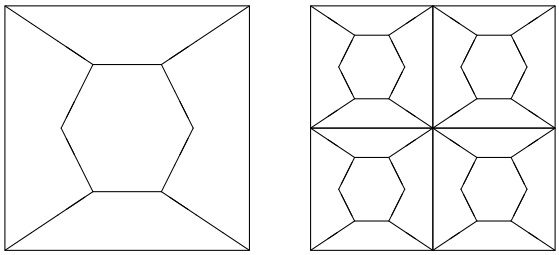

Fig. 2. The level one and level two quadrilateral–pentagonal–hexagonal grids.

Table 1
The error and the order of convergence for (5.1) by $\mathbb{P}_k$ WG finite elements (2.1) on square grids (Fig. 1).

Level	$\|u_h - u\|_0$	Rate	$\|\|\|u_h - u\|\|\|$	Rate
	$\mathbb{P}_1$ element with $\mathbb{P}_2$ gradient ($j = 2$ in (2.2))			
4	0.6829E−03	2.58	0.3218E−01	1.97
5	0.1343E−03	2.35	0.8080E−02	1.99
6	0.3071E−04	2.13	0.2022E−02	2.00
7	0.7483E−05	2.04	0.5056E−03	2.00
	$\mathbb{P}_2$ element with $\mathbb{P}_3$ gradient ($j = 3$ in (2.2))			
4	0.7518E−04	3.93	0.5291E−02	2.97
5	0.5663E−05	3.73	0.6690E−03	2.98
6	0.4687E−06	3.59	0.8390E−04	3.00
7	0.4698E−07	3.32	0.1049E−04	3.00
	$\mathbb{P}_3$ element with $\mathbb{P}_4$ gradient ($j = 4$ in (2.2))			
3	0.3009E−03	6.82	0.9279E−02	4.72
4	0.1304E−04	4.53	0.5598E−03	4.05
5	0.7081E−06	4.20	0.3455E−04	4.02
6	0.3753E−07	4.24	0.2298E−05	3.91
	$\mathbb{P}_4$ element with $\mathbb{P}_5$ gradient ($j = 5$ in (2.2))			
2	0.3124E−01	2.67	0.2036E+00	3.04
3	0.1762E−03	7.47	0.2652E−02	6.26
4	0.1811E−05	6.60	0.5513E−04	5.59
5	0.6090E−07	4.89	0.3395E−05	4.02

for all $v = \{v_0, v_b\} \in V_h^0$, where

$$\langle \frac{1}{h}(u_0 - u_b), v_0 - v_b \rangle_{\partial T_h} = \sum_{T \in \mathcal{T}_h} \int_{e \subset \partial T} \frac{1}{h}(u_0 - u_b)(v_0 - v_b) ds. \tag{5.3}$$

The computation is performed on a PC with an Intel i5-7200U CPU at 2.50 GHz. We list the total CPU time for the two methods in Table 3. The differences are negligible. But the new method is slightly more accurate than the traditional weak Galerkin finite element. This is because the traditional WG has a penalty term which makes the solution more continuous (both new and the traditional solutions are discontinuous) but less flexible. Of course, the P_2 solutions are much more accurate than the P_1 solutions with less computational time.

Table 2
The error and the order of convergence for (5.1) by $\mathbb{P}_k$ WG finite elements (2.1) on quadrilateral–pentagonal–hexagonal grids (Fig. 2).

Level	$\|u_h - u\|_0$	Rate	$\|\|\|u_h - u\|\|\|$	Rate
	$\mathbb{P}_1$ element with $\mathbb{P}_3$ gradient ($j = 3$ in (2.2))			
3	0.3785E−02	0.92	0.1751E+00	0.94
4	0.1315E−02	1.53	0.8855E−01	0.98
5	0.3692E−03	1.83	0.4418E−01	1.00
6	0.9499E−04	1.96	0.2206E−01	1.00
	$\mathbb{P}_2$ element with $\mathbb{P}_4$ gradient ($j = 4$ in (2.2))			
3	0.1219E−02	1.81	0.1617E−01	1.86
4	0.3427E−03	1.83	0.4533E−02	1.84
5	0.8914E−04	1.94	0.1187E−02	1.93
6	0.2254E−04	1.98	0.3011E−03	1.98
	$\mathbb{P}_3$ element with $\mathbb{P}_5$ gradient ($j = 5$ in (2.2))			
2	0.1024E−02	2.75	0.1865E−01	1.99
3	0.1550E−03	2.72	0.4905E−02	1.93
4	0.1422E−04	3.45	0.6854E−03	2.84
5	0.1489E−05	3.26	0.8820E−04	2.96

Table 3
A comparison of new WG (2.3) and the traditional WG (5.2), for solving (5.1) on square grids (Fig. 1).

Level	$\|u_h - u\|_0$	Rate	$\|\|\|u_h - u\|\|\|$	Rate
	New $\mathbb{P}_1$ WG by (2.3)			
5	0.1343E−03	2.35	0.8080E−02	1.99
6	0.3071E−04	2.13	0.2022E−02	2.00
7	0.7483E−05	2.04	0.5056E−03	2.00
	Total CPU time = 876.28125 s			
	The traditional $\mathbb{P}_1$ WG by (5.2)			
5	0.1489E−03	2.28	0.9474E−02	1.89
6	0.3520E−04	2.08	0.2932E−02	1.69
7	0.8681E−05	2.02	0.1132E−02	1.37
	Total CPU time = 876.09375 s			
	New $\mathbb{P}_2$ WG by (2.3)			
4	0.7447E−04	3.94	0.5288E−02	2.97
5	0.5553E−05	3.75	0.6681E−03	2.98
6	0.4609E−06	3.59	0.8377E−04	3.00
	Total CPU time = 371.625 s			
	The traditional $\mathbb{P}_2$ WG by (5.2)			
4	0.7005E−04	4.00	0.5564E−02	2.96
5	0.5040E−05	3.80	0.7260E−03	2.94
6	0.4027E−06	3.65	0.1024E−03	2.83
	Total CPU time = 372.25 s			

5.2. Example 2

We solve problem (1.1) on square domain $\Omega = (0, 1)^2$ again, where the coefficient function and the exact solution are

$$\kappa(|\nabla u|) = \frac{3 + 2|\nabla u|}{1 + |\nabla u|}, \quad u = (x - x^2)\sin(\pi y). \tag{5.4}$$

The errors and the order of convergence are listed in Tables 4–5 for the computation on two types of grids shown in Figs. 1 and 2, respectively. This function κ satisfies condition (1.2) with $\alpha = 2$ and $\beta = 3$. But this non-linear function has an additional singularity, comparing to that in Example 1, the square-root singularity. This is related to the assumption $\kappa \in W^{k,\infty}(\Omega \times \mathbb{R}^+)$ in Theorem 4.3. Here the singularity is caused by the function $|\nabla u| = \sqrt{u_x^2 + u_y^2}$, whose partial derivatives will blowup as $\nabla u \approx 0$ especially when the order $k > 1$. Due to the loss of regularity of the coefficient κ, the higher order finite element methods do not perform as good as the results in Example 1 (see Tables 4–5).

6. Conclusion

In this paper, we studied the stabilizer-free weak Galerkin methods for a class of second order elliptic boundary value problems of divergence form and with gradient nonlinearity in the principal coefficient. With certain assumption on

Table 4
The error and the order of convergence for (5.4) by $\mathbb{P}_k$ WG finite elements (2.1) on square grids (Fig. 1).

Level	$\|u_h - u\|_0$	Rate	$\|\|\|u_h - u\|\|\|$	Rate
	$\mathbb{P}_1$ element with $\mathbb{P}_2$ gradient ($j = 2$ in (2.2))			
4	0.6126E−03	3.42	0.3214E−01	2.06
5	0.7175E−04	3.09	0.7950E−02	2.02
6	0.1003E−04	2.84	0.1982E−02	2.00
7	0.1721E−05	2.54	0.4952E−03	2.00
	$\mathbb{P}_2$ element with $\mathbb{P}_3$ gradient ($j = 3$ in (2.2))			
4	0.3328E−03	3.95	0.6875E−02	3.00
5	0.2511E−04	3.73	0.8669E−03	2.99
6	0.2382E−05	3.40	0.1095E−03	2.98
7	0.2701E−06	3.14	0.1382E−04	2.99
	$\mathbb{P}_3$ element with $\mathbb{P}_4$ gradient ($j = 4$ in (2.2))			
2	0.7066E−01	0.97	0.3533E+00	1.82
3	0.4185E−02	4.08	0.3976E−01	3.15
4	0.2706E−03	3.95	0.4931E−02	3.01
5	0.2536E−04	3.42	0.6241E−03	2.98
	$\mathbb{P}_4$ element with $\mathbb{P}_5$ gradient ($j = 5$ in (2.2))			
2	0.7508E−01	0.98	0.3588E+00	1.95
3	0.7335E−02	3.36	0.4763E−01	2.91
4	0.6863E−03	3.42	0.6028E−02	2.98
5	0.7295E−04	3.23	0.7777E−03	2.95

Table 5
The error and the order of convergence for (5.4) by $\mathbb{P}_k$ WG finite elements (2.1) on quadrilateral–pentagonal–hexagonal grids (Fig. 2).

Level	$\|u_h - u\|_0$	Rate	$\|\|\|u_h - u\|\|\|$	Rate
	$\mathbb{P}_1$ element with $\mathbb{P}_3$ gradient ($j = 3$ in (2.2))			
3	0.5015E−02	2.09	0.1725E+00	1.01
4	0.1308E−02	1.94	0.8634E−01	1.00
5	0.3324E−03	1.98	0.4319E−01	1.00
6	0.8356E−04	1.99	0.2160E−01	1.00
	$\mathbb{P}_2$ element with $\mathbb{P}_4$ gradient ($j = 4$ in (2.2))			
3	0.4899E−03	3.56	0.1394E−01	2.29
4	0.7084E−04	2.79	0.3275E−02	2.09
5	0.1548E−04	2.19	0.8049E−03	2.02
6	0.3853E−05	2.01	0.2001E−03	2.01
	$\mathbb{P}_3$ element with $\mathbb{P}_5$ gradient ($j = 5$ in (2.2))			
2	0.4760E−02	2.79	0.3883E−01	2.41
3	0.2852E−03	4.06	0.4779E−02	3.02
4	0.1755E−04	4.02	0.5969E−03	3.00
5	0.1114E−05	3.98	0.7501E−04	2.99

the nonlinear coefficient, we showed that the discrete problem has a unique solution. This was achieved by showing the associated operator satisfies certain continuity and monotonicity properties. With the help of these properties, we derived optimal error estimates in the energy norm. We presented several numerical experiments to verify the error estimates.

From the numerical experiments in Section 5, we observed superconvergence in both L^2 and energy error estimates, especially on the rectangular grids (cf. Tables 1 and 4). These phenomena, as well as the effects of numerical quadrature on the approximation will be investigated in future works.

Declaration of competing interest

The authors declare that they have no known competing financial interests or personal relationships that could have appeared to influence the work reported in this paper.

CRediT authorship contribution statement

Xiu Ye: Methodology, Validation. **Shangyou Zhang:** Software, Writing - review & editing. **Yunrong Zhu:** Conceptualization, Formal analysis, Writing - original draft.

Acknowledgments

The first author was supported in part by National Science Foundation Grant DMS-1620016, and the third author was supported in part by National Science Foundation, United States Grant DMS-1319110.

References

[1] Glowinski R. Numerical methods for nonlinear variational problems. New York: Springer-Verlag; 1984.
[2] Seidman TI. A class of nonlinear elliptic problems. J Differential Equations 1985;60(2):151–73.
[3] Feistauer M, Ženíšek A. Finite element solution of nonlinear elliptic problems. Numer Math 1987;50(4):451–75.
[4] Chow SS. Finite element error estimates for non-linear elliptic equations of monotone type. Numer Math 1989;54:373–93.
[5] Houston P, Robson J, Süli E. Discontinuous Galerkin finite element approximation of quasilinear elliptic boundary value problems I: The scalar case. IMA J Numer Anal 2005;25(4):726–49.
[6] Bi C, Lin Y. Discontinuous Galerkin method for monotone nonlinear elliptic problems. Int J Numer Anal Model 2012;9(4):999–1024.
[7] Wang J, Ye X. A weak Galerkin finite element method for second-order elliptic problems. J Comput Appl Math 2013;241:103–15.
[8] Mu L, Wang J, Ye X. Weak Galerkin finite element methods on polytopal meshes. Int J Numer Anal Model 2015;12(1):31–53.
[9] Sun S, Huang Z, Wang C. Weak Galerkin finite element method for a class of quasilinear elliptic problems. Appl Math Lett 2018;79:67–72.
[10] Ye X, Zhang S. On stabilizer-free weak Galerkin finite element methods on polytopal meshes. 2019, arXiv:1906.06634 [Cs Math].
[11] Ye X, Zhang S. A conforming discontinuous Galerkin finite element method: Part II. Int J Numer Anal Model 2020;17(2):281–96.
[12] Necas J. Introduction to the theory of nonlinear elliptic equations. John Wiley & Sons; 1986.
[13] Wang J, Ye X. A weak Galerkin mixed finite element method for second order elliptic problems. Math Comp 2014;83(289):2101–26.